Uniform Color Space Modeled with Cone Responses

Rolf G. Kuehni

DyStar L. P., 9844A Southern Pine Blvd., Charlotte, North Carolina 28226

Received 28 January 1999; accepted 19 June 1999

Abstract: An opponent-color model based on simple subtractions of color-matching functions and found useful for modeling the uniform color space is expressed in terms of cone activity functions approximating those of Smith and Pokorny. Taking into account neuro-physiological information, it is found that two stages are necessary to model the yellowness-blueness function and three steps for the redness-greenness function. The third step is similar to one proposed by Müller and Judd. It provides significantly increased hue discrimination in the spectral region of 470–500 nm. The model is shown to be superior for representing uniform color space compared to those proposed by Guth et al. *and DeValois and DeValois.* © 2000 John Wiley & Sons, Inc. Col Res Appl, 25, 56–63, 2000

Key words: uniform color space; zone model; cone response functions; opponent-color system

INTRODUCTION

In previous communications, color-order systems representing uniform color space have been modeled with an opponent color system based on normalized tristimulus values.[1,2] A simple subtractive model with different powers applied to the chromatic semi-axes provides a surprisingly good fit to visually judged uniform color scales. It is apparent that the selection of the three primaries of the CIE colorimetric system has been fortuitous to result in relatively simple calculations, where greenness-redness at equal luminous reflectance is expressed by X only and yellowness-blueness is expressed by Z only.

However, color-matching functions (CMFs) presumably represent the activities of the underlying cone system and are believed to be linearly related to the cone response functions. It is of interest to express the model in terms of assumed linearly related cone response functions. This may provide, among other things, insight into the perplexing question of the reappearance of red at the short end of the spectrum, and how it may be implemented in the visual system.

SELECTING CONE RESPONSE FUNCTIONS

Cone response functions in the form of König fundamentals have been proposed by several authors, among them Smith and Pokorny,[3] Vos and Walraven,[4] and Stockman, MacLeod, and Johnson.[5] In the former two cases, Judd's modified 1931 color-matching functions have been used as a basis. In the latter case the CIE 10° observer color-matching functions are the basis. For the purposes of this work, cone response functions close to the Smith–Pokorny functions have been derived for the CIE 2° observer by applying their transformation formulas to the standard CIE 2° observer data. In the Smith–Pokorny transformation, the L and M response functions add up to the $\bar{y}$ function at a ratio of 0.66537 to 0.33463. The transformation has been changed to result in an exact 2:1 ratio for the input into the brightness function. The transformation equations have also been normalized to have equal areas under the curves in all cases. This is necessary, so that the origin of the system falls on the equal energy point.

CIE 2° Observer

$$L_2 = (0.15546\bar{x}_2 + 0.54414\bar{y}_2\text{-}0.03287\bar{z}_2)/0.6667$$

$$M_2 = (-0.15454\bar{x}_2 + 0.45509\bar{y}_2 + 0.03274\bar{z}_2)/.3333 \quad (1)$$

$$S_2 = \bar{z}_2$$

where $\bar{x}_2$, $\bar{y}_2$, $\bar{z}_2$ are the CIE 2° observer color-matching functions, L_2,M_2,S_2 are the long, medium, and short wave sensitive cone functions derived from the 2° observer color-matching functions.

The functions are shown in Fig. 1.

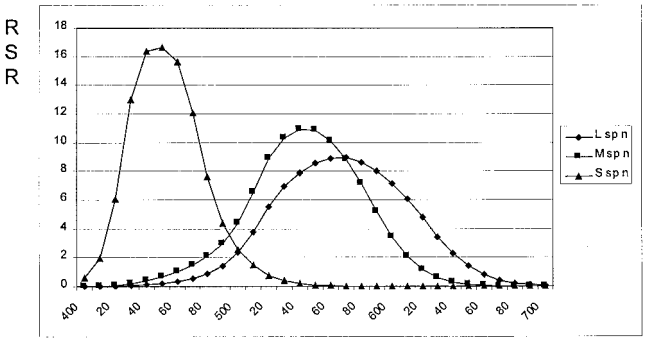

FIG. 1. Cone response functions derived linearly from 2° observer color-matching functions with the Smith–Pokorny transformation equations, normalized to equal areas under the curves. RSR: relative spectral response.

CIE 10° Observer

It is not possible to match the CIE 10° color-matching functions with the Smith–Pokorny cone functions derived from the 2° observer. A number of likely reasons include differences in macular pigmentation, differences in size of the cones, and possible differences in light capture ability. While the difference in the S cones seems to be minor, as judged by the $\bar{z}$ functions of the CIE 2° and 10° standard observers, the $\bar{y}$ (brightness) function of the 10° observer is broader on the short wave side than that of the 2° observer. Cone functions for the 10° observer have been proposed by Stockman, MacLeod, and Johnson as well as by Shapiro, Pokorny, and Smith.[6] Shapiro *et al.* applied the original Smith–Pokorny transformation formula to the 10° observer data. The same has been done for the purposes of this article, except that also here the adjustments discussed under the 2° observer have been applied. The transformation formulas are, thus, the same as shown as (1) except that the 2° observer data have been replaced by the 10° observer data. How the two sets of functions compare is illustrated in Figs. 2 (a)–(c). The difference between the Stockman *et al.* proposed 10° observer cone functions, with the *S* function set equal to $\bar{z}$ as per the suggestion by Schanda[7] and the functions derived from Eq. (1) applied to the 10° observer data is very small and negligible in terms of the work reported in this article.

Based on the equal area under the curve normalization in both cases, perfect matches of the corresponding $\bar{y}$ functions are obtained as follows:

$$\bar{y} = 0.6667\,L + 0.3333\,M. \tag{2}$$

MODELING THE MUNSELL RENOTATION DATA

The modeling of visually uniform global color scale data with *L, M, S* data applicable to the 2° observer is demonstrated with representative selected Munsell Renotation samples.[8] The selection (used also in earlier work[1,2]) involves the hue circle at value 6/chroma 8 and at the same value level colors nearest to the system axes at chroma levels from 2–14 in 2-chroma steps. The locations of these colors in the linearly derived *a, b* diagram, where

$$a = 2.272(X_n - Y_n)$$
$$b = (Y_n - Z_n) \tag{3}$$

with $X_n = X/X_0$ with X_0 being the tristimulus value of the illuminant, etc., are illustrated in Fig. 3. (The magnitude of the multiplier in *a* has been chosen so that the areas under the negative and positive portions of the curve in *a* are the same as in *b*. The value of the multiplier in *a* for the 10° observer is 2.393.) As has been shown in a previous communication, the circularity of this hue circle and the chroma spacing of the colors near the two axes can be much improved by applying different powers to the *a* and *b* axes.[1]

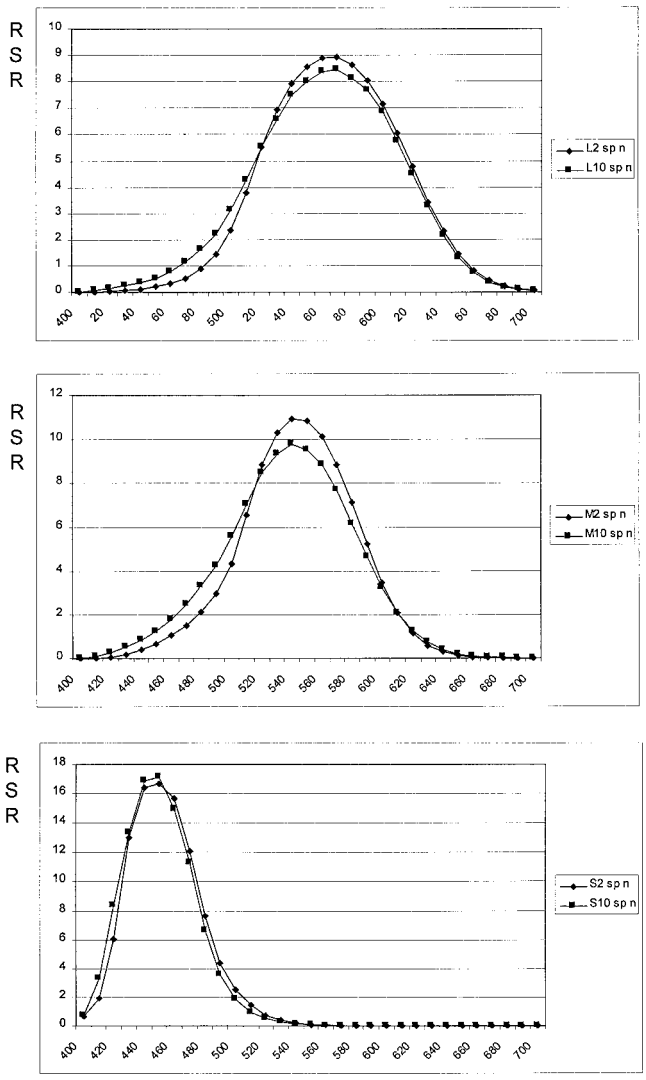

FIG. 2. Comparison of the cone response functions derived from the 10° observer CMFs with those derived from the 2° observer CMFs. (a) *L* function, (b) *M* function, (c) *S* function.

SIGNAL RECORDINGS IN THE GANGLION CELL LAYER AND THE LATERAL GENICULATE NUCLEUS

Lee[9] has reported recordings in cells in the ganglion layer of the retina and the identification of four types of cells that are opponent in character. Bipolar midget cells receive input from M and L cones and their output is either based on $+M-L$ or on $-M+L$. A small bistratified cell type produces a $+S-ML$ signal, and a small bodied inner cell of as yet undetermined input produces a $-S+ML$ signal. Derrington, Krauskopf, and Lennie[10] have reported recordings from parvocellular neurons in the LGN of the macaque monkey and have found opponent-color cells that report data in terms of $L-M$ or the reverse, and in terms of $(L+M)-S$ or the reverse. They appear to be passing on the information generated in the retinal ganglion layer relatively unchanged.

If the data of Fig. 3 are calculated in a comparable manner as balanced "opponent-color" functions:

$$\alpha = 3.807\ (L - M)$$
$$\beta = 0.667\ L + 0.333\ M - S, \tag{4}$$

the plot illustrated in Fig. 4 results. (The equation for β derives from Eq. (3). The multiplier in α is required to adjust the areas under the curve portions to equal size with those in β.) It is apparent that the Munsell yellow-blue color axis is rotated clockwise against the Munsell red-green color axis and does not coincide with the system axis. The output of this system, therefore, is not in agreement with the Hering opponent-color system. It has been a point of discussion by Lee, by Derrington, Krauskopf, and Lennie, as well as several other authors that the "color space" derivable by Eq. (4) is different from the perceptual color space. Lee states: "A complication lies in the relation of cone opponent mechanisms to perceptually opponent colors. . . . Whether it would be sensible to seek for perceptually opponent cells in cortex, or whether this transformation occurs in some kind of neural network remains to be determined; in any event, the locus lies beyond the retina." Derrington, Krauskopf, and Lennie note: "The *B*-(*R&G*) opponent cells must have a major role in color vision . . . . Their axes of best response lie along the constant $R+G$ line; one of the cardinal directions identified in the experiments by Krauskopf *et al.*, but clearly different from the 'unique yellow-unique blue' direction most associated with the activity of the 'yellow-blue' opponent mechanism."*

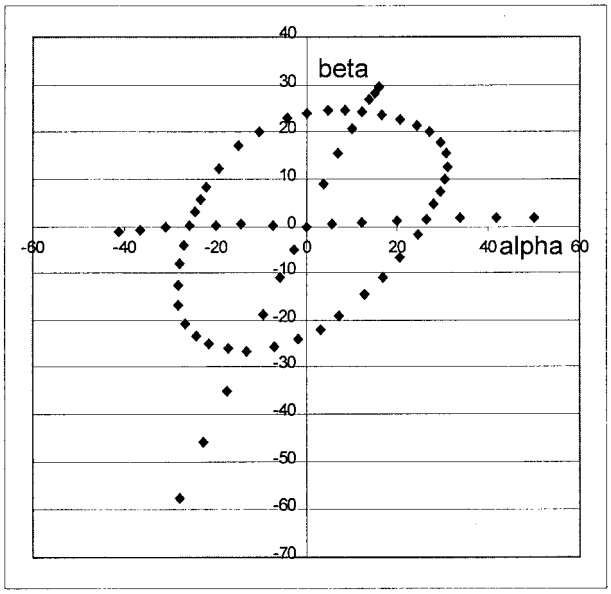

FIG. 4. Plot of the selected Munsell Renotation data from Fig. 3 in the α, β diagram derived from Eq. (4).

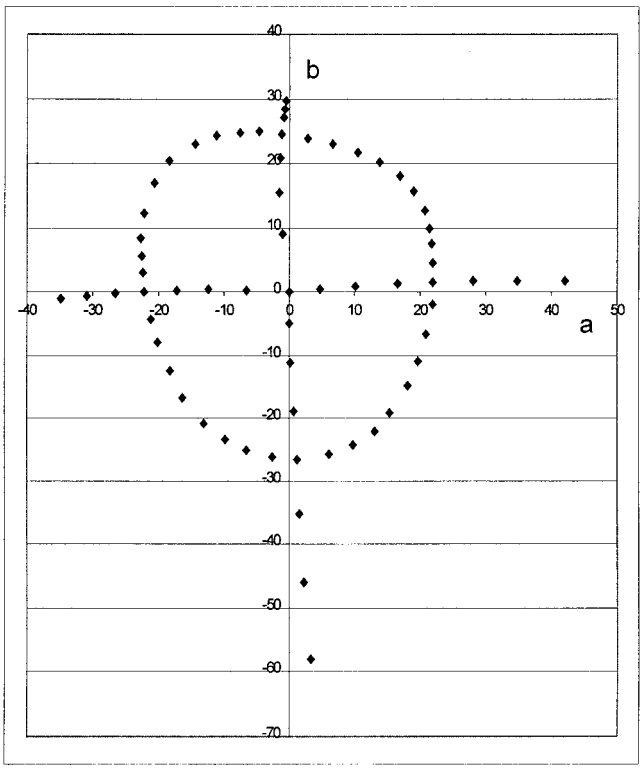

FIG. 3. Selected Munsell Renotation data plotted in the linear *a, b* diagram derived by Eq. (3) from the 2° observer CMFs. Hue circle at value 6 and chroma 8; chroma steps near axes from chroma 2 to chroma 14.

A space based in two dimensions on the above α and β is not a perceptual color space, because the final association between light of a given wavelength and perceived color does not exist yet at this point in the chain of events. It could be termed a "pre-color" space.

It is evident that the Munsell Hue circle colors plotted in Fig. 4 do not, in terms of this pre-color space, have uniform chroma, because their plane vectors are not of equal length. In addition, reddish and greenish hued colors are found on both halves of the diagram. α and β as functions of wavelength are illustrated in Fig. 5.

*In another matter DKL indicate: "It is perhaps worth pointing out that no units in the l.g.n. could be adapted or 'habituated' by prolonged exposure to any of the stimuli used in our experiment." This also indicates that adaptation must be occurring at a level past the LGN.

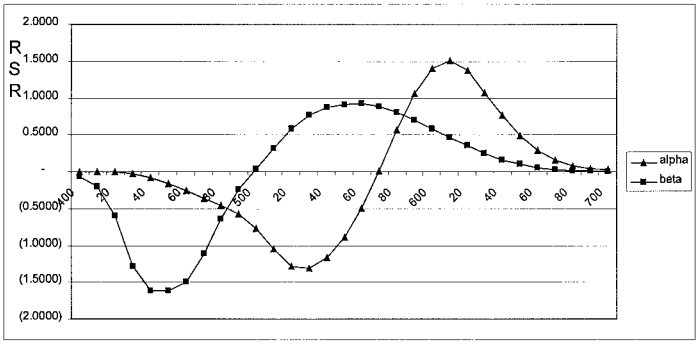

FIG. 5. α and β as a function of wavelength.

a FUNCTION DERIVED FROM *L, M, S*

The solution of how to get from the pre-color space to the color space is built into the color-matching functions. The *a* function of Eq. (3), responsible for redness-greenness, has positive lobes at both ends of the wavelength scale indicating redness in the short- as well as the long-wave region. It can be closely approximated from *L*, *M*, *S* by the following equation:

$$a = 0.231(13L - 15M + 2S). \tag{5}$$

The *b* function is identical to the β function. Plotting the Munsell colors in this *a*, *b* diagram results in a plot nearly identical to Fig. 3. However, Eq. (5) is not a meaningful equation, because we have physiological support for α. So far, we have encountered two stages in the generation of color-related signals: the cone absorption stage and the conversion stage to α and β, resulting in the pre-color space.

Speculation about and proposals for a third stage in color processing have existed since the second half of the last century. An important proposal is by the psychologist Georg E. Müller.[11] He accepted Donders' idea of a zone model[12] and developed at the turn of the century a three-stage model that he refined until the 1930s. His ideas were expressed in 1949 in a model by Judd[13] and further refined in 1970 by Judd and Yonemura.[14] Judd derived three cone functions from the 2° observer data. These are, however, noticeably different from the Smith–Pokorny functions and those of Eq. 1. The second stage involved subtractions somewhat similar to the α and β equations above. In the third stage, the second-stage signals are subtracted with different factors from each other for the redness-greenness signal, while, for the yellowness-blueness, the second-stage signals are added together with different factors. Interestingly, the two chromatic signals, when expressed in terms of color-matching functions, reduce to Eq. (3), however with a factor of 3.16 for the *a* signal.

We have seen that, in the model proposed here, to match the simple linear subtraction of color-matching functions the *b* function remains the same in the second and third stages. The result of Eq. 5 is matched by

$$a = 0.857(\alpha - 0.56\beta). \tag{6}$$

Changing the amount of β in Eq. (6) increases or decreases the size of the short-wave redness lobe. Equation (6), when applied to the Munsell Renotation data, results in a slight curvature of the near-unique blue colors, just as the linear *a* function of Eq. (3) as well as the CIELAB formula does (see Fig. 3). Wright[15] has called the height of the short wavelength lobe of the $\bar{x}$ function exaggerated, and Trezona and Parkins have commented on the lack of solid foundation for the weight distribution of this function.[16] It is evident that modeling of color-order systems can provide input into the proper weight distribution of the $\bar{x}$ function. The curvature is corrected by changing Eq. (6) to

$$a = 0.88(\alpha - 0.50\beta). \tag{7}$$

The result of plotting the Munsell Renotation colors in this slightly modified *a*, *b* diagram is shown in Fig. 6. A comparison of the two versions of *a* is shown in Fig. 7. I will revert to this matter in the next section.

The third stage of processing, where a close approximation of the visually derived hue and chroma relationships of the Munsell system is achieved, therefore consists of the unchanged yellowness-blueness signal of the second stage and the creation of the redness-greenness signal, where the output of a "β" cell is subtracted from the output of two "α" cells. The resulting plot of the Munsell hues is identical to Fig. 3. It should be of considerable interest to search for cells with the behavior of Eq. 7 in the cortex.

$\bar{x}$ AND $\bar{z}$ EXPRESSED IN THE *L,M,S* SYSTEM

With the identity of $\bar{z}$ with *S*, it is evident that at equal luminous reflectance colors changing in yellowness-blueness only cause a change in the activity of the *S* cone. The matter is more complex in the case of redness-greenness. In previous articles, I have shown that at equal luminous reflectance colors changing in redness-greenness only change in X_n.[1,2] However, there is the matter of the required adjustment of the two lobes of the $\bar{x}$ function.

The $\bar{x}$ function is matched by Eq. (6) and approximated by

$$f = 2\,L - 1.2\,M + 0.2\,S. \tag{8}$$

Equation (8) approximately forms the line in the *L*, *M*, *S* space, where at equal luminous reflectance all colors with-

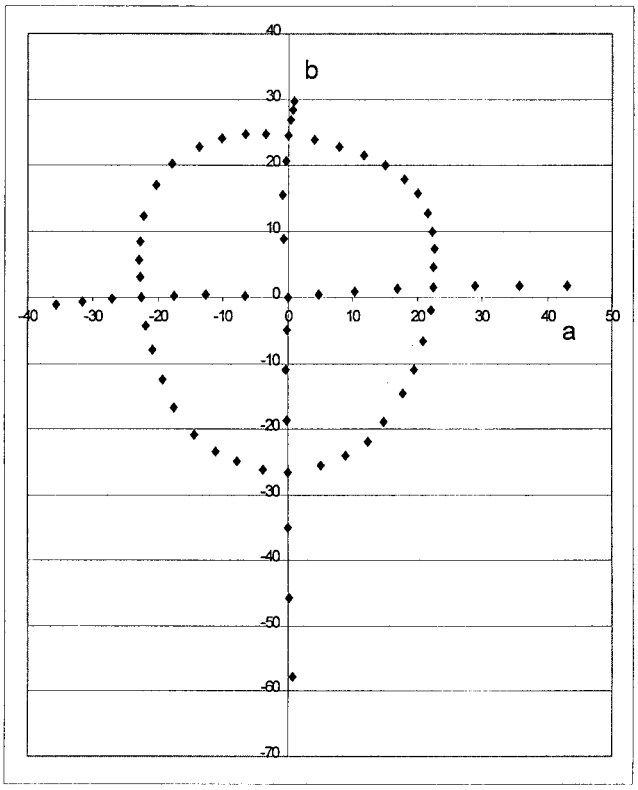

FIG. 6. Plot of the selected Munsell Renotation data from Fig. 3 in the *a, b* diagram derived from Eqs. (7) for *a* and (5) for *b*.

out yellowness-blueness and changing only in redness-greenness are located. When plotting the functions of Eqs. (6) and (7), the former matching the $\bar{x}$ function (see Fig. 6), it is apparent that the two functions differ in a slight redistribution of weight between the two lobes, the redistribution required to eliminate the curvature of bluish and yellowish colors in an *a, b* diagram based on Eq. 3. Equation (7) is, therefore, a more accurate formulation of the line defining the red and green unique hues than $\bar{x}$.

MODELING THE OSA-UCS DATA

The OSA-UCS data are colorimetrically expressed in terms of the 10°observer.[17] With the isotropic structure of the sampling at equal luminance, no explicit hue circle exists in the system. The equiluminant colors at $L = 0$ as expressed in the simple linear system of Eq. (3) (but with the multiplier in *a* of 2.393) are shown in Fig. 8. Also in this case, I have shown previously that significant improvement in the placement of the colors in squares is achieved by applying different powers to the normalized X and Z tristimulus values and by making an adjustment for the imbalance of the $\bar{x}$ function.[1]

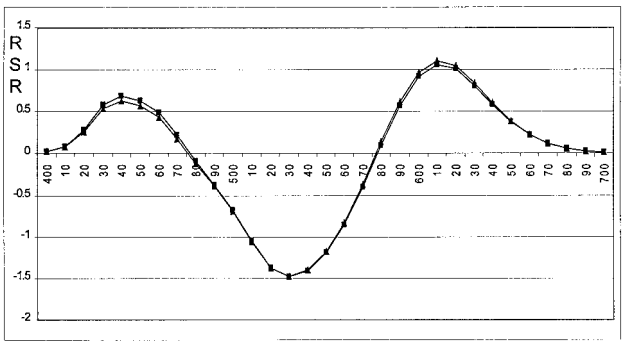

FIG. 7. Comparison of the *a* functions derived from Eqs. (7) (■) and (8) (▲).

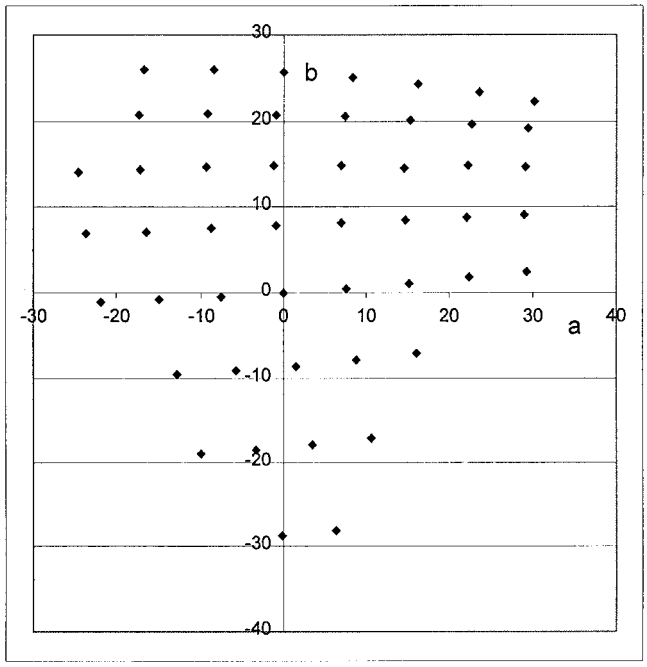

FIG. 8. OSA-UCS colors at $L = 0$ plotted in the linear *a, b* diagram derived with Eq. (3).

The α, β diagram for the 10° observer is obtained in a manner very similar to that for the 2° observer. The relationships are as follows:

$$\alpha = 3.777\ (L - M)$$
$$\beta = (0.6667\ L + 0.3333\ M - S) \tag{9}$$

The result of plotting the colors of Fig. 8 in this diagram is shown in Fig. 9, with results comparable to those of Fig. 4.

The rotated *a* function is calculated in an identical manner to that of Eq. (6):

$$a = 0.908(\alpha - 0.56\ \beta). \tag{10}$$

Equation (10) matches the *a* function derived from subtracting the color-matching functions. Also in this case, adjustment for the curvature of the near-unique hue yellow and blue colors is required. It is achieved in a manner analogous to that of Eq. (7):

$$a = 0.933\ (\alpha - 0.50\ \beta). \tag{11}$$

When plotting the OSA-UCS $L = 0$ colors in this *a, b* diagram, as shown in Fig. 10, the result is improved over

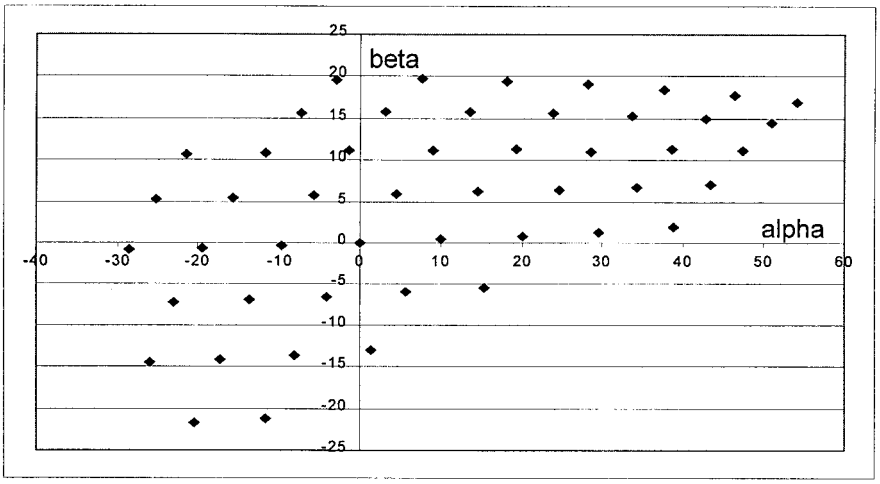

FIG. 9. OSA-UCS colors at $L = 0$ plotted in the α, β diagram of the 10° observer.

that of Fig. 8. Further improvement is obtained, as mentioned, by applying different power functions to *a* and *b.*

COMPARISON WITH OTHER MODELING APPROACHES

To my best knowledge, uniform color space data have not before been modeled in terms of cone response functions. Opponent-color models have been proposed by other authors. Among these are Guth and co-workers,[18] De Valois and De Valois,[19] and Wandell.[20] In the Guth model chromatic functions *T* and *D* are calculated based on Smith–Pokorny cone response functions. However, the *T* function is calculated only at the α level. The results with the Munsell test data are, therefore, comparable to those of Fig. 4.

DeValois and DeValois have made a comprehensive proposal of a three-stage color model. They used Smith–Pokorny cone response functions, however, in a form where the maximum value of each function is 1. In the second stage, so-called cone opponency functions were calculated where $L_0 = L - (L+M+S)$ and comparably for the other two functions. In the third stage, perceptual opponency functions are calculated. The complete transformation is equal to

$$\begin{aligned} a &= 18L - 23M + 5S \\ b &= -26L + 19M + 7S \end{aligned} \tag{12}$$

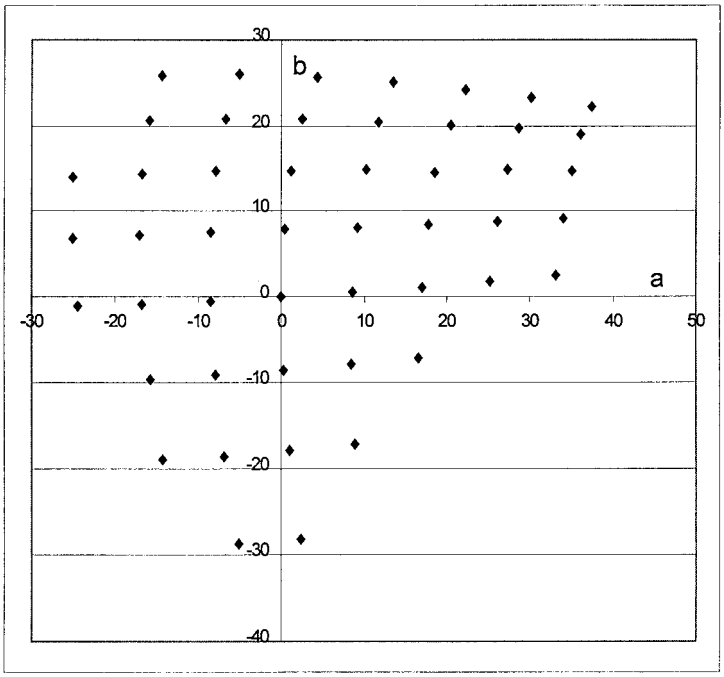

FIG. 10. OSA-UCS colors at α, β diagram plotted in the *a, b* diagram derived with Eq. (11) for *a* and (9) for *b*.

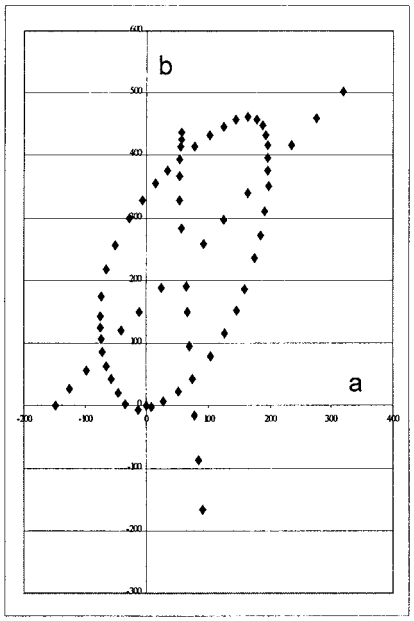

FIG. 11. Munsell Renotation colors in the *a, b* diagram derived from DeValois and DeValois' multi-stage color model equations.

The Munsell test colors as expressed in this system are illustrated in Fig. 11. It is apparent that the system is not balanced.

In his book, *Foundations of Vision*, Wandell has provided a transformation formula for Smith–Pokorny cone sensitivity functions (normalized to the maximum value being 1) that decorrelates the *L, M, S* signals as calculated for the Macbeth Color Checker[21] colors. Of the resulting three functions, one is equal to *L* and two are similar to *a* and *b*. The Munsell test colors plotted in this diagram are shown in Fig. 12. The formula has not been presented by Wandell as a recommendation for a color model. However, it is interesting to see how close chromatic functions derived from mathematical decorrelation of the *L, M, S* signals resulting from 18 chromatic and 6 achromatic colors are to simple subtractive functions of the color-matching functions.

It was of interest to also show the Munsell test colors in the basis model behind the new CIECAM97 chromatic adaptation formula.[22] This formula uses a transformation to cone functions that are much different from the Smith–Pokorny functions. The chromatic signals are then calculated somewhat similar to Eq. (5) for *a* and Eq. (4) for *b*:

$$a = R - 12G/11 + B/11$$
$$b = (1/9)(R + G - 2B). \tag{13}$$

The results are shown in Fig. 13.

DISCUSSION

Analysis of uniform color space as represented by two color-order systems, one expressed in terms of the 2° observer the other in terms of the 10° observer, offers surprisingly simple ratios of cone activation to model the perceptual systems quite closely. The result is a 2-1/2 stage zone model, where only the redness-greenness signal requires a third stage. The final stage in the redness-greenness signal is modeled again with a simple subtraction mechanism. This further subtraction step provides considerable additional hue discrimination in the short wave area. At the α,β level, unique blue would be located at the short-wave end of the spectrum or perhaps be extra-spectral, like unique red. From the zero crossing point of the β function towards the short wave end of the visible spectrum, there would only be greenish blue hues with increasingly less greenishness. Assuming equal relative change in *a* and *b* to be responsible for equal hue steps, it is apparent that there would be significantly fewer steps in the seemingly critical region between approximately 470–500 nm. In place of about 11 Munsell 40 hue type steps there would only be 7. The change from α *to a* represents a more than 50% increase in hue discrimination in this area. It can be assumed that a genetic mutation resulting in this change proved to be of evolutionary benefit.

It is well known that examining the Munsell Book of Colors or the OSA-UCS color atlas represents a limited activity of our color vision system. It is, nevertheless, one that applies in practice quite closely, if we evaluate colored materials or their color differences under controlled conditions, and it may not be radically different from observing an average natural scene outdoors. It is, therefore, not surprising that relatively simple opponent-color models can describe this situation with good accuracy.

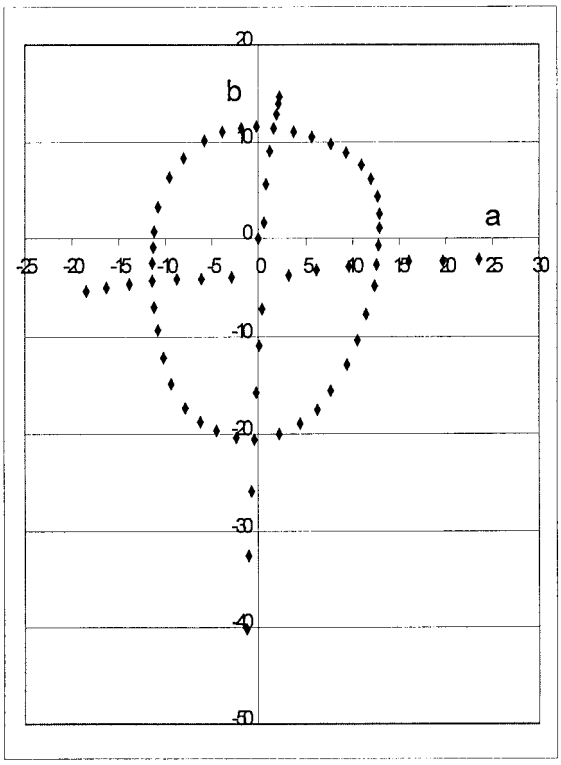

FIG. 12. Munsell Renotation colors in the *a, b* diagram derived from Wandell's Color Checker *L, M, S* decorrelation equations.

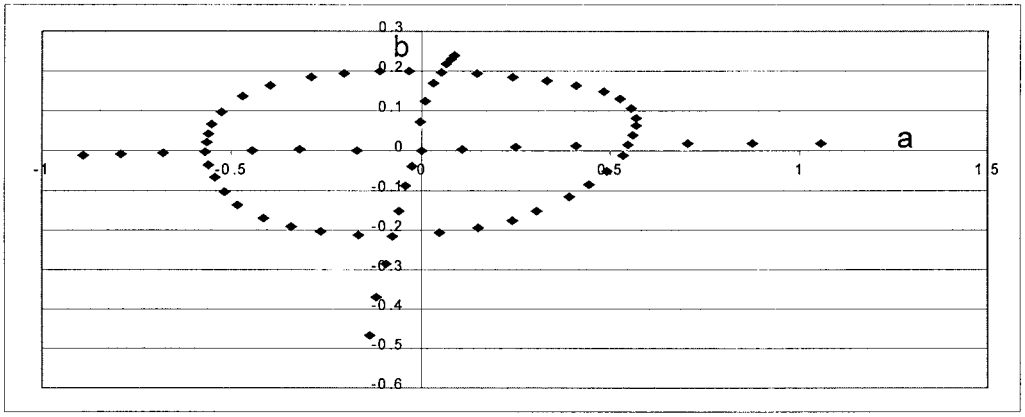

FIG. 13. Munsell Renotation colors in the *a, b* basis diagram of the CIECAM97s color-appearance model.

CONCLUSION

When expressing the spacing of visually uniform color samples with a colorimetric model, good fits are obtained with cone sensitivity functions derived linearly from the corresponding color-matching functions as proposed for example by Smith and Pokorny. Building a zone model that is in agreement with certain neuro-physiological findings requires two steps for the yellowness-blueness function and three steps for the redness-greenness function. The third step is similar to one proposed early in the century by G. E. Müller and appears to involve a simple subtraction of the second step signals. The result of this subtraction has considerable impact on information discrimination in the 470–500 nm region of the spectrum.

1. Kuehni RG. Towards an improved uniform color space. Col Res Appl 1999;24:253–265.
2. Kuehni RG. A comparison of five color order systems. Col Res Appl, to appear.
3. Smith VC, Pokorny J. Spectral sensitivity of the foveal cone photopigments between 400 and 500 nm. Vision Res 1975;15:161–171.
4. Vos JJ, Walraven PL. On the derivation of the foveal receptor primaries. Vision Res 1971;11:791–818.
5. Stockman A, MacLeod DIA, Johnson NE. Spectral sensitivities of the human cones. J Opt Soc Am A 1993;10:2491–2521.
6. Shapiro AG, Pokorny J, Smith VC. Cone-rod receptor spaces with illustrations that use CRT phosphor and light-emitting-diode spectra. J Opt Soc Am A 1996;13:2319–2328.
7. Schanda J. Current CIE work to achieve physiologically correct color metrics. In: Backhaus WGK, Kliegl R, Werner JS, editors. Color vision. Berlin: De Gruyter; 1998. p 307–318.
8. Munsell renotations. In: Wyszecki G, Stiles WS, editors. Color science. 2nd Ed. New York: Wiley; 1982.
9. Lee BB. Receptors, channels and color in primate retina. In: Backhaus WGK, Kliegl R, Werner JS, editors. Color vision. Berlin: De Gruyter; 1998. p 79–88.
10. Derrington AM, Krauskopf J, Lennie P. Chromatic mechanisms in lateral geniculate nucleus of macaque. J Physiol 1984;357:241–256.
11. Müller GE. Über die Farbenempfindungen. Z Psychol Ergänzungsb 1930; p 17, 18.
12. Donders FC. Über Farbensysteme. Archiv f Opthalm 1881;26:155–223.
13. Judd DB. Response functions for types of vision according to the Müller theory. J Res Nat Bur Standards (Washington DC) 1949; 42:1.
14. Judd DB, Yonemura GT. CIE 1960 UCS diagram and the Müller theory of color vision. J Res Nat Bur of Standards 1970;74A:23–30.
15. Wright WD. The measurement of color. 4th Ed. New York: Van Nostrand Reinhold; 1969. p 124.
16. Trezona PW, Parkins RP. Derivation of the 1964 colorimetric standards. Col Res Appl 1998;23:221–225.
17. OSA-UCS data. In: Wyszecki G, Stiles WS, editors. Color science. 2nd Ed. New York: Wiley; 1982.
18. Guth SL, Massof RW, Benzschawel T. Vector model for normal and dichromatic color vision. J Opt Soc Am A 1980;8:197–211.
19. DeValois RL, DeValois KK. A multi-stage color model. Vision Res 1993;33:1053–1065.
20. Wandell B. Foundations of vision. Sunderland: Sinauer; 1995.
21. Macbeth color checker. Windsor, NY: Gretag Macbeth; 2553–6148.
22. Luo MR, Hunt RWG. The structure of the CIE 1997 colour appearance model. Col Res Appl 1998;23:138–146.